Available online at www.sciencedirect.com
ScienceDirect
Composites: Part B 39 (2008) 83–91
composites Part B: engineering
www.elsevier.com/locate/compositesb

The high strain rate response of PVC foams and end-grain balsa wood

V.L. Tagarielli, V.S. Deshpande, N.A. Fleck *

Cambridge University, Engineering Department, Trumpington Street, Cambridge, CB2 1PZ, UK

Available online 16 February 2007

Abstract

The uniaxial compressive responses of two polymeric foams (Divinycell H100 and H250) and balsa wood (ProBalsa LD7) have been measured over a wide range of strain rates, ranging from 10^{-4} s^{-1} to 4000 s^{-1}. These materials are widely used as cores for composite sandwich structures. The high strain rate compression tests were performed using a Split-Hopkinson Pressure Bar made from AZM magnesium alloy, with semi-conductor strain gauges used to measure the low levels of stress in the specimens. The experimental data for compressive strength as a function of strain rate are adequately approximated by power-law fits. The compressive yield strength of the H250 PVC foam and balsa wood doubles when the strain rate is increased from quasi-static rates (10^{-4} s^{-1}) to rates on the order of 10^{3} s^{-1}. In contrast, the H100 PVC foam displays only a small elevation in uniaxial compressive strength (about 30%) for the same increase in strain rate.

Keywords: A. Foams; A. Wood; B. Mechanical properites; Strain rate sensitivity

1. Introduction

Polymeric foams and balsa wood have widespread applications as core materials in composite sandwich structures for marine applications. Demand has grown for lightweight structures capable of providing impact and blast protection and this has stimulated research on the dynamic response of composite sandwich structures with PVC foam and balsa wood cores.

An understanding of the mechanical response of lightweight cellular solids at high rates of strain is needed in order to investigate the overall dynamic performance of sandwich structures. Though the static deformation mechanisms of PVC foams and balsa wood are well understood, only limited experimental data exist on the high strain rate responses these cellular materials. The objective of this study is to measure the strength of PVC foams and balsa wood in uniaxial compression at low and high strain rates. This data can then be used to calibrate dynamic constitutive models used in numerical simulations of the dynamic response of composite sandwich structures with PVC foam and balsa wood cores. This is dealt with in a separate publication [1].

The outline of this paper is as follows. First, the static mechanisms of collapse of PVC foams and balsa wood in uniaxial compression are examined, the physical basis of the strain rate sensitivity of cellular solids is discussed, and experimental studies on the dynamic compressive response of cellular materials are reviewed. Second, the experimental techniques are described for measuring the uniaxial compressive response of PVC foams and balsa wood at strain rates in the range 10^{-4} s^{-1}–4000 s^{-1}. And third, the experimental results are reported and the observed strain rate sensitivity is discussed in the context of the existing literature.

1.1. Static collapse of cellular solids in uniaxial compression

The mechanics of cellular materials have been comprehensively discussed by Gibson and Ashby [2]. These authors have developed micromechanical models which

* Corresponding author. Tel.: +44 (0) 1223 332650; fax: +44 (0) 1223 332662.
E-mail address: naf1@eng.cam.ac.uk (N.A. Fleck).

1359-8368/$ - see front matter © 2007 Elsevier Ltd. All rights reserved.
doi:10.1016/j.compositesb.2007.02.005

relate the macroscopic mechanical properties of the cellular material with its parent material properties and topology.

Isotropic, open-celled foams have a low connectivity per node (of the order 6) and deform by plastic bending of the cell walls. Consequently, the macroscopic compressive plateau strength $\sigma_{\rm pl}$ of the foam is related to the yield strength of the strut material $\sigma_{\rm Ys}$ by

$$\sigma_{\rm pl} = C\bar{\rho}^{3/2}\sigma_{\rm Ys}, \tag{1}$$

where $\bar{\rho}$ is the relative density of the foam (defined as the ratio of foam density to that of the cell-wall material) and C is a proportionality constant, of order unity, with precise value depending upon the details of the foam microstructure [2]. Regardless of whether the foam is open-celled or closed-cell, a dimensional analysis dictates that the macroscopic compressive strength of the foam scales linearly with the yield strength of the constituent solid. Similarly, the local strain rate in cell walls of the foam also scales linearly with the macroscopic applied strain rate.

The above observations hold for isotropic or nearly isotropic foams. Prismatic 2D cellular solids such as honeycomb and balsa wood are highly anisotropic and the deformation mechanisms are strongly dependent on the direction of deformation. When the material is compressed along the direction of the elongated cells, these collapse by a combination of axial yield of the cell walls followed by local plastic buckling, similar to the progressive plastic collapse observed in the axial loading of circular tubes. On the other hand, if these materials are compressed in the transverse direction, plastic bending of the cells walls is the dominant deformation mechanism. A dimensional analysis again dictates that the macroscopic compressive strength $\sigma_{\rm pl}$ scales linearly with the yield strength of the cell-wall material $\sigma_{\rm YS}$ and likewise, the macroscopic strain rate $\dot{\varepsilon}$ scales linearly with the local strain rate in the cell walls $\dot{\varepsilon}_{\rm S}$. These linear relations are written mathematically as

$$\sigma_{\rm pl} = K_\sigma(\bar{\rho})\sigma_{\rm Ys}; \quad \dot{\varepsilon} = K_{\dot{\varepsilon}}(\bar{\rho})\dot{\varepsilon}_{\rm s}, \tag{2}$$

where K_σ and $K_{\dot{\varepsilon}}$ denote proportionality constants for a given microstructure and relative density $\bar{\rho}$, i.e., K_σ and $K_{\dot{\varepsilon}}$ are functions of $\bar{\rho}$. For example Deshpande and Fleck [3] have shown that $K_{\dot{\varepsilon}} \approx 10$ for a bending-governed cellular material with a cubic microstructure.

1.2. Physical basis of the strain rate sensitivity of cellular solids

Studies on the dynamic properties of cellular materials such as foams, wood and honeycombs, have attributed the strength increase under dynamic loading conditions to a series of concurrent factors. Here we briefly review the physical phenomena that contribute to the strain rate sensitivity of cellular materials, and discuss their relevance in governing the high strain rate response of PVC foams and balsa wood.

1.2.1. Strain sensitivity of the cell-wall material

A degree of strain rate sensitivity is expected in the foams from the inherent strain rate sensitivity of the parent material. For example, assume that the strain rate sensitivity of the cell-wall material is given by a power law relation of the form

$$\sigma_{\rm Ys} = K_{\rm s}\dot{\varepsilon}_{\rm s}^{m}, \tag{3}$$

where $K_{\rm s}$ is proportionally constant and $m_{\rm s}$ the power law exponent. Substituting (3) in (2), we obtain the strain rate sensitivity of the cellular solid as

$$\sigma_{\rm pl} = K\dot{\varepsilon}^{m} \text{ where } K = K_\sigma K_{\rm s} K_{\dot{\varepsilon}}^{-m}. \tag{4}$$

Thus, if no other dynamic effects are active, we expect the strain rate sensitivity of the foam to have the same power law exponent as that of the solid parent material. Of course, the value of the proportionality constant K depends on the foam relative density and topology.

1.2.2. Micro-inertial effects

The micro-inertia of individual cell walls can affect the deformation modes of cellular solids, as discussed by Klintworth [4]. Under dynamic loading, the collapse mode of a bending-governed cellular material may switch from the quasi-static mode to a new mode involving additional cell-wall stretching, which dissipates more energy and hence leads to an increase in the collapse strength.

This phenomenon has been investigated by Calladine and English [5] for two classes of structures, referred to as 'Type I' and 'Type II' structures. Type I structures have a 'flat-topped' quasi-static compressive stress versus strain response: under dynamic loading, micro-inertia plays little role and the quasi-static bending mode of collapse is maintained. In contrast, Type II structures display a strongly softening mode of collapse under quasi-static conditions. When Type II structures are struck at high velocities, lateral inertia forces induce an initial phase of axial compression of the structure. Consequently, the stresses and plastic work are enhanced before the bending mechanism is recovered and these structures have an inertia sensitive response.

We note that PVC foams are nearly isotropic and behave as Type I structures with a nearly "flat-topped" compressive stress versus strain response, see for example [3]. Thus, it is expected that micro-inertial effects will play only a minor role in enhancing the dynamic strength of these foams. By contrast, balsa wood compressed in the direction of the elongated cells (the "axial" direction of the material, which coincides with the axis of the tree trunk), behaves as a Type II structure with a softening compressive stress versus strain response – experimental findings of Reid and Peng [6] seem to support this hypothesis.

1.2.3. Shock-wave propagation

If a cellular material is impacted at high velocity, a plastic shock wave will propagate through the solid. This plastic wave propagation phenomenon leads to an increase

of the collapse strength of the material, which can be quantified considering a simple one-dimensional shock model [7].

Consider the uniaxial compression of a foam at a constant velocity V. The compression generates a shock wave traveling from the end where the velocity is imposed to the opposite fixed end. If the foam has a rigid-perfectly plastic static response up to the densification strain ε_D, it can be shown that the stress ahead of the shock-wave equals the yield strength of the material σ_{pl}, whereas the stress σ_D upstream from the shock is given by

$$\sigma_D = \sigma_{pl} + \frac{\rho_f V^2}{\varepsilon_D}, \quad (5)$$

where ρ_f is the density of the foam. Hence, an elevation of $\rho_f V^2/\varepsilon_D$ is expected in the compressive strength of the material.

For a typical PVC foam (Divinycell[1] H250) we can assume that $\rho_f \approx 250\ \mathrm{kg\ m^{-3}}$, $\varepsilon_D \approx 0.8$ and $\sigma_{pl} \approx 6$ MPa. We conclude that shock wave propagation effects become important (i.e., static strength is enhanced by more than 20%) for compression velocities $V > 60\ \mathrm{m\ s^{-1}}$. In this study, we limit ourselves to velocities less than $20\ \mathrm{m\ s^{-1}}$ and hence expect that shock wave propagation plays only a minor role in governing the dynamic response of the cellular materials.

1.3. Review of literature on the strain rate sensitivity of PVC foams and wood

The experimental techniques for measuring the response of materials at high rates of strain are well established. Typically the Split-Hopkinson pressure bar (SHPB) is employed to measure the stress versus strain responses of solids in compression [8], tension [9] or torsion [10] for strain rates in the range $10^2\ \mathrm{s^{-1}} \leqslant \dot{\varepsilon} \leqslant 10^4\ \mathrm{s^{-1}}$. The SHPB has been extensively employed to measure the strain rate sensitivity of solid polymeric materials such as PVC, PC and PMMA (see for example, [11–13]). In line with their visco-elastic nature, these polymeric materials exhibit a strong strain rate sensitivity with the yield strength increasing by about 50–200% when the strain rate is increased from $10^{-4}\ \mathrm{s^{-1}}$ to $10^3\ \mathrm{s^{-1}}$.

Although the dynamic testing of structural materials (such as metallic alloys and engineering plastics) using the SHPB is routine, soft solids such foams and wood have received much less attention. The paucity of data is primarily related to difficulties associated with conducting SHPB tests on soft solids. Most of the studies on soft solids used either aluminium Hopkinson bars [14] or magnesium bars as in [15].

The strain rate sensitivity of PVC foams with densities in the range $75\ \mathrm{kg\ m^{-3}}$–$300\ \mathrm{kg\ m^{-3}}$ has been investigated by Chakravarty et al. [16], and Thomas et al. [17]. Their measured data is summarised in Fig. 1 along with the measured strain rate sensitivity of solid PVC [11] (the data in Fig. 1 has been labelled using the designations used in [16,17] and consists of one or two letters, followed by a number which is the density of the foam in $\mathrm{kg\ m^{-3}}$). We note that the R300, H130 and HD130 display a strain rate sensitivity similar to that of the solid PVC while the R75 foam is nearly strain rate insensitive over the range $10^{-4}\ \mathrm{s^{-1}} \leqslant \dot{\varepsilon} \leqslant 10^4\ \mathrm{s^{-1}}$.

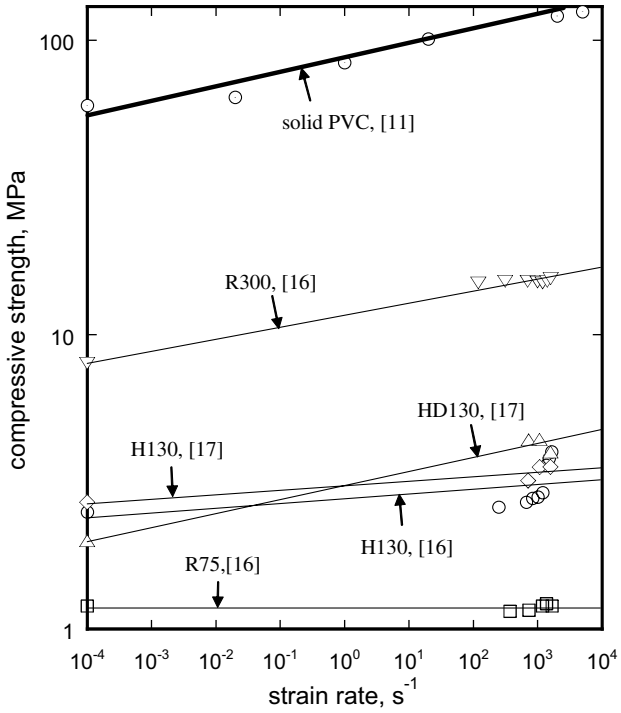

Fig. 1. A summary of the strain rate sensitivity of solid PVC and PVC foams. The data plotted here is taken from the literature and fitted by the power law relation (18). The foams are identified by their trade names which comprise a letter or letters followed by the density of the foam in $\mathrm{kg\ m^{-3}}$.

Wood is one of the oldest structural materials and its dynamic response has been addressed by several researchers, see for example Johnson [18], in which historical studies on the microstructure of wood and its use as a shock absorber are reviewed. A comprehensive experimental study on the dynamic response of a number of varieties of wood, including balsa, pine and oak, was conducted by Reid and Peng [6]. In this study, dynamic compression tests were conducted by firing circular cylindrical specimens at an instrumented Hopkinson pressure bar, at velocities ranging from $10\ \mathrm{m\ s^{-1}}$ to $300\ \mathrm{m\ s^{-1}}$. In these tests, the specimens were relatively long (typically 45 mm). Thus, shock wave effects dominate for impact velocities exceeding about $90\ \mathrm{m\ s^{-1}}$ and hence it is difficult to extract the inherent material strain rate sensitivity from the results of Reid and Peng [6].

2. Materials

Divinycell PVC foams and end-grain balsa wood were obtained in the form of plates with nominal thickness rang-

[1] DIAB AB, Box 201, 312 22 Laholm – Sweden.

ing from 5 mm to 16 mm. The Divinycell PVC foams are designated H100 (density 100 kg m^{-3}) and H250 (density 250 kg m^{-3}), whereas the end-grain balsa wood used was ProBalsa LD7 (nominal density 90 kg m^{-3}). All materials were supplied by DIAB.

Preliminary checks revealed that Divinycell foams are approximately isotropic, and their density is uniform across the foam plates. The microstructure of these materials comprises closed-cells, with an average cell size of about 350 μm for the H100 foam and 180 μm for the H250 foam. Balsa wood is transversely isotropic, with the isotropic plane perpendicular to the axis of the tree [19,20]. On the scale of millimetres and above, balsa wood is a cellular solid made up of long, prismatic cells with pointed ends. The diameter of the cells is about 50 μm, and the cells have a length to diameter ratio of about 15. They resemble hexagonal honeycombs in shape, and are subdivided occasionally by transverse walls. In all experiments reported in this study, balsa specimens are compressed along the direction of the trunk of the tree, that is, along the direction of the elongated cells. The density of the balsa wood plates is not uniform since the plates were manufactured by gluing together discrete blocks selected at random. The density varies from 70 kg m^{-3} to 130 kg m^{-3} across the sheets supplied by DIAB.

3. Experimental investigation

3.1. Low strain rate tests

Compression tests were performed on the H100 and H250 PVC foams and on the balsa wood at a nominal strain rate of 10^{-4} s^{-1} using a screw-driven test machine. The compressive load was measured by the load cell of the test machine, while the compressive strain was deduced from the relative displacement of the compression platens, measured via a laser extensometer. The platens were lubricated with a silicone spray to reduce friction.

Cuboidal specimens of cross-section of 30 mm × 30 mm and thickness of 5–16 mm were employed in these tests. For the case of the balsa wood, care was taken to ensure that the specimens did not span the glued interfaces of the plates, so that the measured properties represent true balsa wood properties. All balsa specimens were cut from blocks with a density of about 70 kg m^{-3} in order to ensure a consistent set of results.

3.2. Intermediate strain rate tests

In order to achieve strain rates of 0.01–250 s^{-1}, uniaxial compression tests were conducted using a servo-hydraulic test machine, at compression speeds of up to 1.5 m s^{-1}. The load was measured by the load cell of the test machine, and the specimen shortening was determined via the LVDT displacement sensor of the machine. In order to prevent damage to the machine upon impact of the loading platens, the tests were arrested at a nominal compressive strain of about 70%. This strain level was adequate for capturing the initial elastic phase, plateau regime and partial densification of the two PVC foams. However, only the elastic phase and the plateau regime were recorded for the balsa wood specimens.

These intermediate strain rate compression experiments were performed on circular cylindrical specimens, (this specimen geometry was also used in the high strain rate tests detailed below). The circular cylindrical specimens were cut from sheets of the PVC foams and balsa wood using a metallic punch of internal diameter 12.7 mm. The thickness of the specimens was 4.89 mm and 4.86 mm for the H100 and H250 PVC foams, respectively, while the balsa specimens were of thickness 6.83 mm. A low aspect ratio was chosen for these specimens, in order to minimise the time required to achieve force equilibrium along the axis of the specimen in the high strain rate compression tests. Silicon spray was again applied to loading platens the specimens in order to reduce friction during the compression tests.

3.3. High strain rate compression test

High compressive strain rates, ranging from 500 s^{-1} to 4000 s^{-1}, were achieved with a Split-Hopkinson Pressure Bar (SHPB). This apparatus, comprising AZM magnesium alloy bars, was developed for measuring the dynamic compressive response of soft solids such as mammal skin and rubber [15], and is sketched in Fig. 2.

A striker bar of length 0.4 m, and input and output bars of length 1.0 m were used. All bars were made from 12.7 mm diameter AZM magnesium alloy rods. The magnesium alloy (density 1800 kg m^{-3}) was chosen in order to attain a high sensitivity in the stress measurement. Recall that magnesium alloys have a low value of Young's modulus ($E = 44$ GPa) and this results in a relatively large

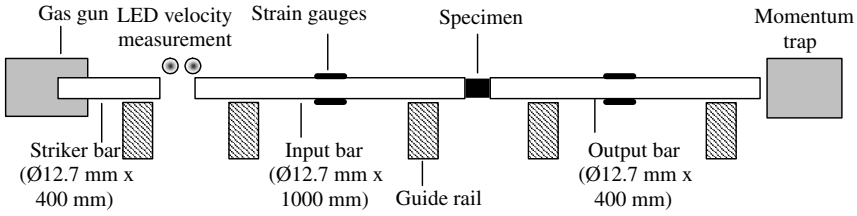

Fig. 2. Sketch of a compressive Split-Hopkinson pressure bar apparatus used for testing soft materials (reproduced from [15]).

axial strain due to the transient axial loading of the bar by the soft foams and balsa wood. Magnesium alloy is preferred to polymeric materials to avoid the complications of dispersion and attenuation of the stress waves as they propagate along the polymer bar [21].

The SHPB was operated as follows. A striker bar was accelerated along the barrel of a gas gun by pressured nitrogen gas (gas pressure of 0.05–0.1 MPa). The striker bar velocity (2–20 m s^{-1}) was measured using two light sensors at a spacing of 50 mm. The velocity of the striker was limited to about 20 m s^{-1} in order to ensure that the magnesium alloy did not yield during the tests.

The cylindrical specimen was sandwiched between the input and output bars. Impact of the striker bar against the end of the input bar caused an elastic compression wave (incident wave) to propagate along the input bar. The resulting displacement of the input bar compressed the specimen. A small fraction of the compression wave was transmitted through the specimen and into the output bar, whilst the remainder was reflected back along the input bar as a tensile wave.

The axial strain in the input bar and output bar was measured by two semi-conductor strain gauges bonded diametrically opposite to each other, and mid-way along the length of each bar. Semi-conductor strain gauges were preferred to conventional foil gauges as they have a gauge factor of 140, whereas foil gauges have a gauge factor of about 2. The strain gauge readings were used to determine the stress versus strain response of the specimen, as detailed below.

The strain gauges were connected in series with a 2200 Ω resistor, as shown in Fig. 3. The axial strain was detected by measuring the change in the voltage across this series resistor (note that the two strain gauges are in series, which results in the strains due to bending of the bars being eliminated). An oscilloscope measured and recorded the voltage versus time response during the compression tests. The data were downloaded from the oscilloscope to a PC and stored for subsequent analysis.

Fig. 4 shows an example of the axial strain signal in the input and output bars, for the case of a H250 PVC foam specimen and striker bar velocity of 13.4 m s^{-1}. The imposed nominal strain rate in this test is 2760 s^{-1}. The

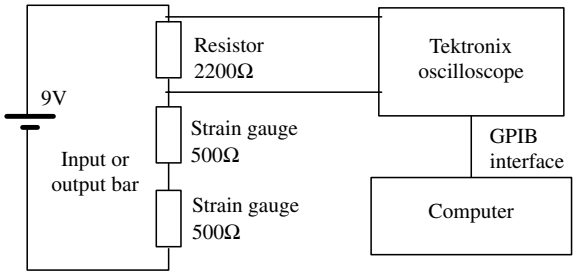

Fig. 3. Sketch of the circuit used for measuring the strain in the pressure bars by recording the change in the voltage across a resistor (reproduced from [15]).

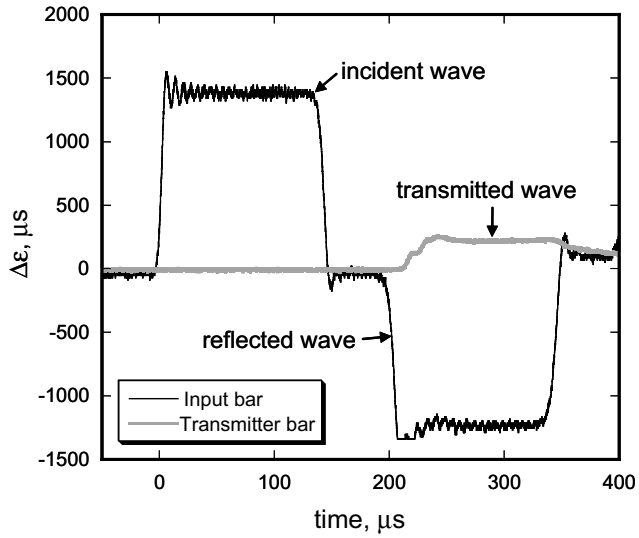

Fig. 4. The strain recorded in the incident and transmitter pressure bars for the case of a H250 foam specimen tested at a strain rate of 2760 s^{-1} (striker velocity of 13.4 m s^{-1}). Time $t = 0$ corresponds to the instant of the impact of the striker bar on the incident bar. The incident, reflected and transmitted pulses are indicated in the figure.

incident and reflected pulses are recorded by the gauges on the input bar, whereas the grey curve is the transmitted pulse, as recorded by the strain gauge on the output bar. Observe that the incident and reflected pulses are approximately rectangular in shape, as expected by one-dimensional wave theory.

3.3.1. Calibration of the SHPB system

A dynamic calibration of the strain gauges was performed on the SHPB system. The strain pulse generated by impact of the striker bar upon the input bar is recorded by the strain gauges on the input bar. Simple momentum considerations and wave theory dictate that the amplitude of this strain pulse equals

$$\varepsilon = \frac{V_0}{2c_s}, \tag{6}$$

where V_0 is the striker bar velocity and c_s is the longitudinal wave propagation speed in the bar material. The corresponding level of stress is given by

$$\sigma = E\varepsilon = \frac{EV_0}{2c_s} = \frac{\rho c_s V_0}{2}, \tag{7}$$

where ρ is the bar material density and E Young's modulus of the bar material. The change in voltage recorded by the strain gauges is directly proportional to the strain in the bar

$$\Delta V = \alpha\varepsilon. \tag{8}$$

Eqs. (6) and (7) were used to calculate the proportionality constant α and convert the change in voltage recorded by the strain gauges directly into axial strain, and thereby into axial stress. For the bar system employed in this study, it was found that $\alpha = 460$ V.

Observe that Eqs. (6) and (7) involve the longitudinal wave speed in the input and output bars. This speed was measured by timing the passage of the incident and reflected pulses on the strain gauges on the input bar. For the magnesium bars, the longitudinal wave propagation speed was measured as 4950 m s^{-1}, in line with the calculated value of

$$c_s = \sqrt{\frac{E}{\rho}} = 4940 \text{ m s}^{-1}. \tag{9}$$

3.3.2. Theory of measurements

According to one-dimensional theory of elastic wave propagation, the axial displacement $u(t)$ at time t is related to the axial strain history $\varepsilon(t)$ by

$$u(t) = c_s \int_0^t \varepsilon(t) d\tau. \tag{10}$$

It follows that the axial displacement at the interface between the input bar and the specimen is given by

$$u_1 = c_s \int_0^t (\varepsilon_I - \varepsilon_R) d\tau, \tag{11}$$

and similarly, the displacement of the interface between the specimen and the output bar is

$$u_2 = c_s \int_0^t \varepsilon_T d\tau. \tag{12}$$

The nominal compressive strain in the specimen can be calculated as

$$\varepsilon_s(t) = \frac{u_1 - u_2}{L_s} = \frac{c_s}{L_s} \int_0^t (\varepsilon_I - \varepsilon_R - \varepsilon_T) d\tau, \tag{13}$$

where L_s is the initial length of the specimen. The axial loads on the incident and distal ends of the specimen are given by

$$F_1 = EA(\varepsilon_I + \varepsilon_R), \tag{14a}$$

and

$$F_2 = EA\varepsilon_T, \tag{14b}$$

respectively, where A is the cross-section of the input and output bars. The two forces can be out of balance due to shock-wave effects within the specimen. Fig. 5 presents the variation of the forces in the input and output bar with time, for the case of a H250 specimen tested with a striker velocity of 6.0 m s^{-1}; the associated nominal strain rate is 1240 s^{-1}. The two forces are not equal initially, but approach each other as the wave pulse is reflected back and forth within the specimen. Force equilibrium in this test is reached after 30–40 μs.

Force equilibrium implies that $\varepsilon_T \approx \varepsilon_I + \varepsilon_R$, and Eq. (13) simplifies to

$$\varepsilon_s = -\frac{2c_s}{L_s} \int_0^t \varepsilon_R d\tau. \tag{15}$$

The strain rate in the specimens is then given by

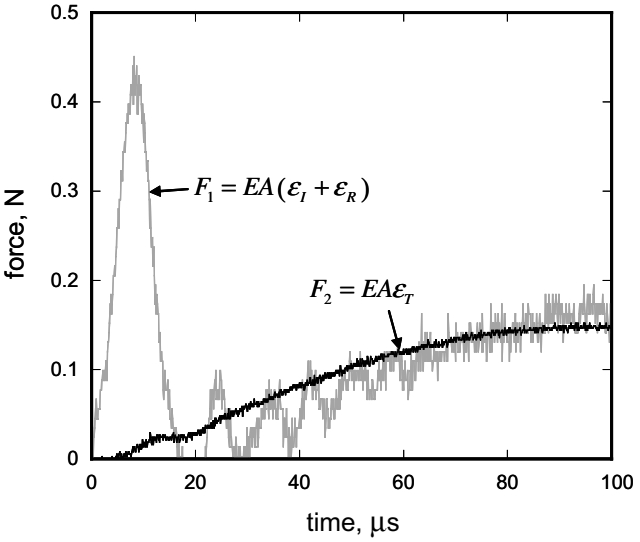

Fig. 5. The time histories of the forces on the incident and distal ends of a H250 foam specimen, compressed at a strain rate of 1240 s^{-1} (striker velocity of 6.0 m s^{-1}) in the SHPB apparatus. Time $t = 0$ corresponds to the instant that the compression wave in the incident bar reaches the specimen.

$$\dot{\varepsilon}_s = -\frac{2c_s}{L_s} \varepsilon_R, \tag{16}$$

while the nominal compressive stress in the specimen is

$$\sigma_s = E\left(\frac{A}{A_s}\right)\varepsilon_T, \tag{17}$$

where A_s is the cross-sectional area of the specimen.

4. Results and discussion

The plateau strength σ_{pl}, defined as the stress at a total strain of 15%, was extracted from the engineering stress

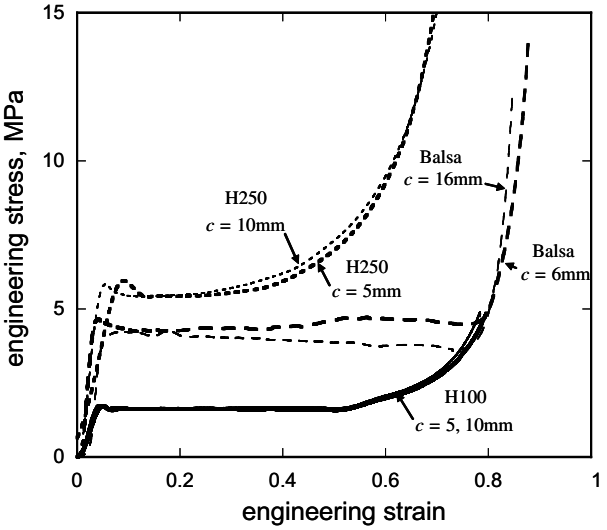

Fig. 6. Quasi-static ($\dot{\varepsilon} = 10^{-4}$ s^{-1}) uniaxial compressive stress versus strain responses of the two PVC foams (H100 and H250) and the balsa wood. For each material, the engineering stress versus engineering strain responses are reported for two choices of the specimen thickness.

versus strain curves and was recorded as a function of strain rate for the three materials. Shock wave effects can be neglected since, for all tests conducted in this study, the impact velocity was sufficiently low for the inertial stresses (scaling with $\rho_f V^2$) to be much less than the plateau strength σ_{pl}. Thus, the dynamic strength enhancements of the plateau strength σ_{pl} reported below are due to the intrinsic strain rate sensitivities of the materials.

4.1. Compressive response at low strain rates

Fig. 6 presents a summary of the static uniaxial compressive responses for the three materials, measured at a strain rate of $10^{-4}\,s^{-1}$. The figure includes the measured engineering stress versus strain curves for the Divinycell H100 foam (specimens of thickness 5 and 15 mm), H250 foam (specimens of thickness 5 and 10 mm) and ProBalsa LD7 balsa wood (specimens of thickness 6 and 16 mm). In all cases, the material exhibits an initial elastic regime, followed by a plateau phase and densification.

The static compressive strength of the materials σ_{pl}, arbitrarily defined as the stress at a total strain of 15%, was found to be 1.7, 5.8 and 4.5 MPa for the H100, H250 and balsa wood, respectively, in line with the properties reported in the manufacturer's data sheets and independent of the specimen thickness. The nominal densification strain was 80% for the H100 and the balsa wood, and about 70% for the H250 PVC foam. While balsa wood displays a flat plateau region up to densification, the PVC foams exhibit some hardening before densification. Almost no lateral expansion was observed in the plastic range in any of the compression tests.

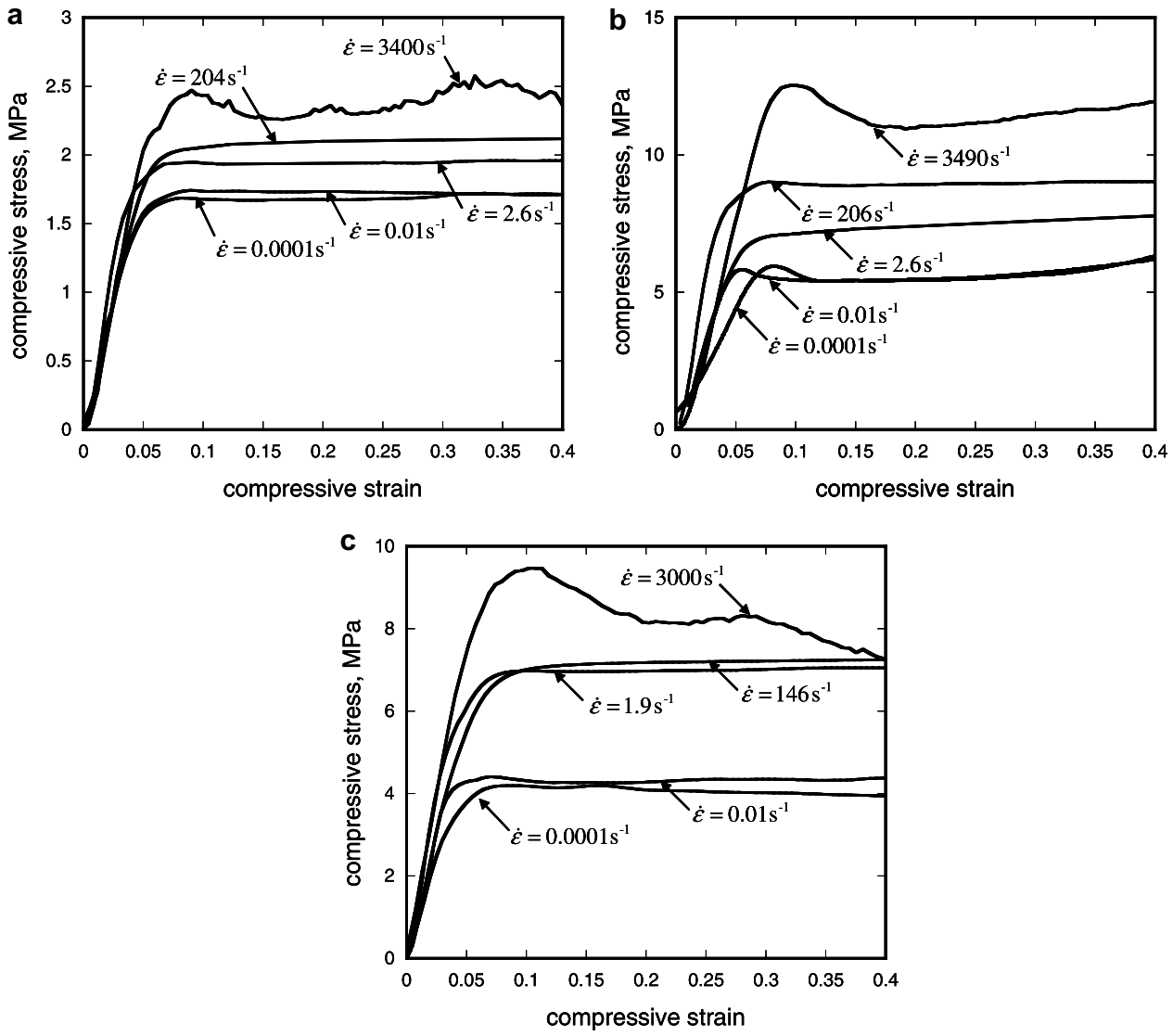

Fig. 7. A comparison between the measured static, intermediate and high strain rate compressive responses of the (a) H100 PVC foam, (b) H250 PVC foam and (c) balsa wood.

4.2. Compressive response at higher strain rates

A comparison between the static ($\dot{\varepsilon} = 10^{-4}$ s^{-1}) intermediate (10^{-2} s$^{-1} \leqslant \dot{\varepsilon} \leqslant 250$ s^{-1}) and high strain rate (500 s^{-1} $\leqslant \dot{\varepsilon} \leqslant 4000$ s^{-1}) responses of the three materials under investigation is presented in Fig. 7. Observe that data obtained for strain rates higher than 10^2 s^{-1} have been filtered in order to reduce instrumentation noise. For all the materials and strain rates examined here, the uniaxial compressive response comprises an elastic phase, in which stress increases linearly with strain, and a plastic plateau phase where the stress is constant or mildly increasing with the applied strain. Post-test observation revealed negligible lateral expansion of the specimens, confirming that the plastic Poisson's ratios are close to zero for the three materials in dynamic compression.

An elevation of the plateau strength $\sigma_{\rm pl}$ with the applied strain rate is evident from comparing the stress versus strain curves in Fig. 7. For the H250 foam (Fig. 7b) and the balsa wood (Fig. 7c), this elevation is of about 100% over the range of strain rates considered, whereas the elevation of $\sigma_{\rm pl}$ is of about 30% for the H100 foam (Fig. 7a). Note that the stress versus strain curves obtained from SHPB experiments on balsa wood (see for example the curve in Fig. 7c at $\dot{\varepsilon} = 3000$ s^{-1}) display a softening post-yield response. It is argued that this is due to fracture of the balsa specimens, as detected from post-test observations.

Fig. 8 summarises the results obtained in this study. The figure shows the dependence of the plateau strength upon strain rate, for all three cellular materials. Note that data scattering of about 20% on the plateau strength is typically observed in these experiments; at each value of the applied strain rate, the compression tests were repeated three times, and the plateau strength plotted in Fig. 8 is the average of the three measured values. For strain rates $\dot{\varepsilon} > 0.01$ s^{-1}, the measured $\sigma_{\rm pl}$ versus $\dot{\varepsilon}$ relation is adequately described by a power law relation of the form

$$\frac{\sigma_{\rm pl}}{\sigma_0} = \left(\frac{\dot{\varepsilon}}{\dot{\varepsilon}_0}\right)^m, \tag{18}$$

where $\dot{\varepsilon}$ is a reference strain rate, σ_0 a reference stress, and m is the power law exponent. With the reference strain rate $\dot{\varepsilon}_0 = 1$ s^{-1}, a least-squares fit to the experimental data provides the coefficients and m. These values are listed in Table 1 and the corresponding fits are included in Fig. 8.

The data in Fig. 8 reveals that the PVC foams and balsa wood display negligible strain rate sensitivity for strain rates in the range 10^{-4} s^{-1} $\leqslant \dot{\varepsilon} \leqslant 10^{-2}$ s^{-1} but display a power law strain rate sensitivity at higher strain rates. Moreover, the power law exponent m for the H250 PVC foam is approximately equal to that measured for solid PVC by Walley and Field [11], see Table 1. This confirms our hypothesis in Section 1 that the strain rate sensitivity of the PVC foams is mainly governed by that of the parent material. By contrast, the H100 foam displays markedly lower strain rate sensitivity than that of solid PVC. An investigation into the physical origins of this behaviour is beyond the scope of this study. However, it is worth mentioning here that Subhash et al. [22] have reported that the strain rate sensitivity of epoxy-based foams increases with increasing relative density of the foam (i.e., the power law exponent m increases with increasing $\bar{\rho}$) and the present findings for PVC foams are consistent with this trend.

We finally compare the strain rate sensitivities for the PVC foams measured in this study with those reported in the literature. The data of Chakravarty et al. [16] and Thomas et al. [17] for the R75, H130 and R300 foams from Fig. 1 is replotted in Fig. 8 (dashed lines). We note that strain rate sensitivity of the R300 foam [16] is similar to that of the H250 foams investigated in this study, while the strain rate sensitivity of the H100 foam studied here is intermediate to the R75 [16] and H130 [17] foams. This confirms that the decrease in strain rate sensitivity of the PVC foams with decreasing density is consistent with previous investigations on PVC foams.

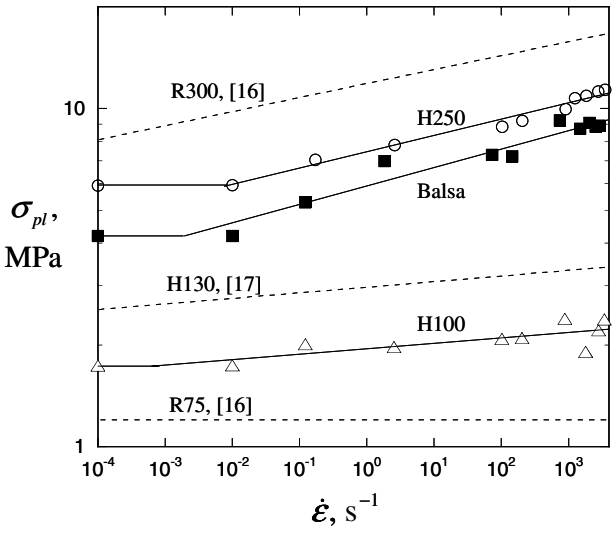

Fig. 8. Summary of the strain rate sensitivity of the plateau strength (defined as the flow stress at a total strain of 15%) of the cellular materials tested in this study. The data is fitted with the power law relation (18) and the coefficients are listed in Table 1. For comparison purposes, the relevant data from the literature (Fig. 1) is re-plotted here with dashed lines.

Table 1
The power-law coefficients ((18)) employed to fit the experimental data for the PVC foams and balsa wood in Fig. 8

	σ_0	m
H100	1.95	0.016
H250	7.44	0.048
Balsa	5.87	0.056
Solid PVC[11]	86.85	0.050

The coefficients used to fit the solid PVC data of Walley and Field [11] are also included in this table. In all cases a reference strain rate $\dot{\varepsilon}_0 = 1$ s^{-1} is chosen.

5. Concluding remarks

The uniaxial compressive stress versus strain responses of two PVC foams (Divinycell H100 and H250) and end-grain balsa wood (Probalsa LD7) have been measured over a wide range of strain rates. A screw-driven test machine was used for low strain rates ($10^{-4}\ s^{-1}$), whereas a servo-hydraulic test machine was used for strain rates of up to $500\ s^{-1}$. A purpose-built split pressure Hopkinson bar, constructed from magnesium alloy and employing semi-conductor strain gauges to measure the bar strain, was able to detect the low stresses in these soft solids at strain rates within the range 500–4000 s^{-1}.

The experiments revealed that the compressive response of the cellular materials under investigation is mildly strain rate sensitive in the range $\dot{\varepsilon} = 10^{-2}$–$4 \times 10^{3}\ s^{-1}$, whereas negligible strain rate sensitivity is observed for $\dot{\varepsilon} = 10^{-4}$–$10^{-2}\ s^{-1}$. Thus, quasi-static tests can give misleading information on strain rate sensitivity over the full range of strain rates.

For the H250 PVC foam and the LD7 balsa wood, the plateau strength increased by a factor of two with respect to the static strength, at strain rates of the order of $10^{3}\ s^{-1}$, whereas the compressive response of the H100 PVC foam was only mildly affected by high rates of straining, displaying an elevation of the compressive strength of about 30% at strain rates of the order of $10^{3}\ s^{-1}$.

Acknowledgements

This work was financially supported by the EPRSC (Engineering and Physical Sciences Research Council) and ONR (US Office of Naval Research), Contract number 0014-91-J-1916, program manager Dr. Yapa Rajapakse.

References

[1] Tagarielli VL, Deshpande VS, Fleck NA. Dynamic collapse of composite sandwich beams: analytical and finite element predictions, Int J Solids Struct [in press].
[2] Gibson LJ, Ashby MF. Cellular solids, structure and properties. 2nd ed. Cambridge: Cambridge University Press; 1997.
[3] Deshpande VS, Fleck NA. High strain rate compressive behaviour of aluminium alloy foams. Int J Impact Eng 2000;24:277–98.
[4] Klintworth JW. Dynamic crushing of cellular solids. PhD thesis, Department of Engineering, University of Cambridge; 1989.
[5] Calladine CR, English RW. Strain-rate and inertia effects in the collapse of two types of energy absorbing structures. Int J Mech Sci 1984;26(11–12):689.
[6] Reid SR, Peng C. Dynamic uniaxial crushing of wood. Int J Impact Eng 1997;19(5–6):531–70.
[7] Harrigan JJ, Peng C, Reid SR. Inertia effects in impact energy absorbing materials and structures. In: Langseth M, Krauthammer T, editors. Proceedings of transient loading and response of structures, International symposium honouring Mr. Arnfinn Jenssen. Norwegian Defence Construction Service and Department of Structural Engineering, Norwegian University of Science and Technology, TAPIR:Trondheim; 1998. p. 447. ISBN: 82-7482-044-4. See also Int J Impact Eng 1999;22(9–10):965.
[8] Kolsky H. An investigation of the mechanical properties of materials at very high rates of loading. Proc Phys Soc (London) 1949;62B: 676–700.
[9] Harding J, Wood EO, Campbell JD. Tensile testing of materials at impact rates of strain. J Mech Eng Sci 1960;2:88–96.
[10] Duffy J, Campbell JD, Hawley RH. On the use of a torsional split Hopkinson Bar to study rate effects in 1100-O Aluminium. J Appl Mech (Trans ASME) 1971;38:83–91.
[11] Walley SM, Field JE. Strain rate sensitivity of polymers in compression from low to high strain rates. DYMAY J 1994;1(3):211–27.
[12] Fleck NA, Stronge WJ, Liu JH. High strain-rate shear response of polycarbonate and polymethyl methacrylate. Proc R Soc Lond A 1990;429:459–79.
[13] Chen W, Lu F, Cheng M. Tension and compression tests of two polymers under quasi-static and dynamic loading. Polym Test 2002; 21:113–21.
[14] Chen W, Lu F, Frew DJ, Forrestal MJ. Dynamic compression testing of soft materials. J Appl Mech-Trans ASME 2000;69(3):214–23.
[15] Shergold OA, Fleck NA, Radford D. The uniaxial stress versus strain response of pig skin and silicone rubber at low and high strain rates, Int J Impact Eng [in press].
[16] Chakravarty U, Mahfuz H, Saha M, Jeelani S. Strain rate effects on sandwich core materials: An experimental and analytical investigation. Acta Mater 2003;51(5):1469–79.
[17] Thomas T, Mahfuz H, Kanny K, Jeelani S. High strain rate response of cross linked and linear PVC cores. J Reinf Plastics Compos 2004;23(7):739–49.
[18] Johnson W. Historical and present-day references concerning impact on wood. Int J Impact Eng 1986;4:175–83.
[19] Easterling KE, Harrysson R, Gibson LJ, Ashby MF. On the mechanics of balsa and other woods. Proc R Soc Lond 1982;A383: 31–41.
[20] Tagarielli VL, Deshpande VS, Fleck NA, Chen C. A transversely isotropic model for foams, and its application to the indentation of balsa. Int J Mech Sci 2005;47:666–86.
[21] Bacon C. Separation of waves propagating in an elastic or viscoelastic Hopkinson pressure bar with three-dimensional effects. Int J Impact Eng 1999;22(1):55–69.
[22] Subhash G, Liu Q, Gao X. Quasistatic and high strain rate uniaxial compressive response of polymeric structural foams. Int J Impact Eng 2005;32(7):1113–26.